Int. J. Multiphase Flow Vol. 14, No. 4, pp. 413–424, 1988
Printed in Great Britain.

0301-9322/88 $3.00 + 0.00

CHORD LENGTH DISTRIBUTIONS RELATED TO BUBBLE SIZE DISTRIBUTIONS IN MULTIPHASE FLOWS

N. N. CLARK[1] and R. TURTON[2]

Departments of [1]Mechanical and Aerospace Engineering and [2]Chemical Engineering, West Virginia University, Morgantown, WV 26506, U.S.A.

(*Received* 25 *September* 1986; *in revised form* 22 *January* 1988)

Abstract—Generally, if a probe is used to measure the size of a bubble or void in a multiphase system, the probe intersects the bubble with a chord length other than the diameter of the largest vertical chord length of the bubble. This matter is further complicated by the fact that there is a distribution of bubble sizes in most systems. From geometric reasoning, the expected probability distribution of measured chord sizes from a given bubble diameter is deduced and the relationship between bubble size distributions and chord length distributions explored. All one need know to evaluate these relationships is the fundamental bubble shape.

Key Words: two-phase (flow), bubble, shape, probe, size distribution, gas–liquid (flow), fluidization

INTRODUCTION

Probes are used widely in the study of multiphase systems, particularly gas–liquid flows and fluidized beds. One use of probes is to measure the diameter of bubbles in the system. This measurement may be made directly using dual hydrostatic pressure probes (Atkinson & Clark 1986a, 1987) provided that pressure distributions around the bubble are known. Otherwise, chord length can be inferred using a single probe, such as a resistance probe in gas–liquid flows and bubble columns (Serizawa *et al.* 1975; Sekoguchi *et al.* 1975; Burgess *et al.* 1981; Koide *et al.* 1979) if the velocity of the bubble is known. Pairs of probes, situated one downstream of the other in the direction of bubble movement, employing data processing, have also been used in gas–liquid systems (Herringe & Davis 1978). Optical probes have been used in a similar fashion to resistance probes to measure multiphase flow properties (Galaup 1975; Buchholz *et al.* 1981), while Flemmer (1984) has proposed and tested a new type of pneumatic probe to detect voids in fluidized beds. Probes have been discussed in more detail in reviews by Gunn & Al-Doori (1985), Atkinson & Clark (1986b), Werther & Molerus (1973), Cheremisinoff (1986) and Fitzgerald (1979), and in the thesis of Galaup (1975).

In all of these probe measurements, the probes do not always intersect the bubble at its center: a chord length smaller than the largest vertical bubble dimension is typically measured. This paper relates the distribution of chord lengths measured to the size distribution of bubbles affecting the probe and offers techniques for transforming the chord length distribution into the actual bubble diameter distribution. Most previous studies have considered only average chord lengths in the system and have not related the two distributions—this is discussed by Cheremisinoff (1986). Exceptions are Yamashita *et al.* (1979), who presented an analysis similar to that developed below for bubbles which approximate canted ellipsoids, and Werther & Molerus (1973) and Werther (1974a, b), who analyzed capacitance probe signals in fluidized beds.

ANALYSIS

Consider a swarm of gas bubbles rising through a liquid or dense phase medium. A probe is operated amidst the bubbles. Let the size distribution of bubbles *which intersect the probe* be given by the probability density function $P(R)$. Note that this distribution of bubble sizes *touching* the probe is not equal to the distribution of bubble sizes *in the system*, $P_s(R)$, because, all else being equal, the larger the bubble size the greater will be the number of bubbles which influence the probe. These two distributions are related by a weighting function, proportional to R^2. Further work in this paper refers to both of these distributions, which must be distinguished carefully by the reader.

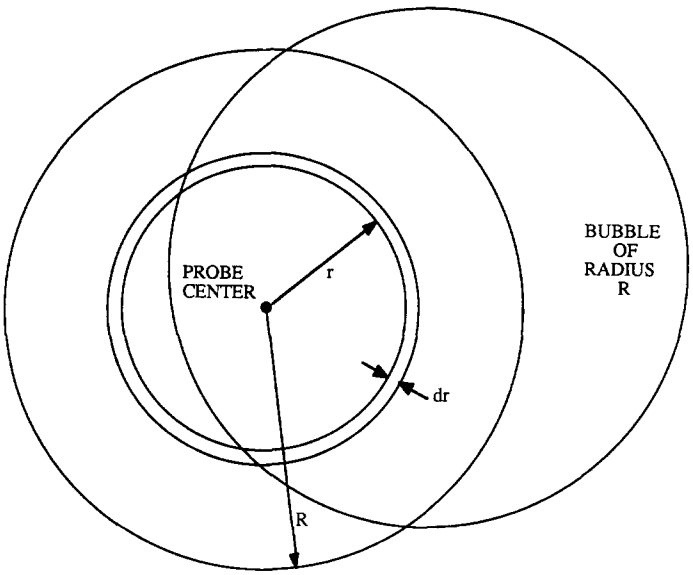

Figure 1. View from above of a bubble of radius R rising past a probe. The bubble will intersect the probe if its center is a distance $< R$ from the probe.

Now consider the interaction of bubbles of a particular size, R, with the probe tip. Let the center of one of these bubbles be a distance, r, from the probe tip, as shown in figure 1. This bubble will intersect the probe tip if r lies between zero and the radius of the bubble, R. A large number of bubbles of size R intersect the tip over a long period of time and it is assumed that bubble centers are uniformly distributed throughout the system, or at least within a cylinder of radius R from the probe tip. Therefore, over a long period of time, the number of bubble centers passing through a small annulus dr wide and radius r from the probe tip increases in direct proportion to r. We conclude that the probability density function for the distance between bubble centers and the probe tip is in direct proportion to the distance r. Hence,

$$P(r \mid R) = ar, \qquad 0 \leqslant r \leqslant R,$$
$$P(r \mid R) = 0, \qquad \text{otherwise.} \tag{1}$$

$P(r \mid R)$ is a conditional distribution of r given a value of R. The function $P(r \mid R)$, when integrated over some range of r, is effectively the number of bubbles of size R intersecting the probe at a distance in that range, divided by the total number intersecting the probe. Since $P(r \mid R)$ is a probability density function, a has the value $2/R^2$.

Next, we must assume some functional size-independent shape for the bubbles. This allows us to predict the vertical chord length, y, that the probe will cut for a given value of r. We assume that all bubbles rise vertically (see figure 2).

Since

$$y = f(r) \tag{2}$$

we can determine the probability density function which describes the likelihood of finding a chord length y for a specified bubble size R:

$$P(y \mid R) = P(r \mid R)\left|\frac{\mathrm{d}r}{\mathrm{d}y}\right|$$
$$= \frac{2r}{R^2}\cdot\left|\frac{\mathrm{d}r}{\mathrm{d}y}\right|. \tag{3}$$

The integral of $P(y \mid R)$ over all possible chord lengths for bubbles of specified size R must be unity. The analysis offered thus far applies to a population of bubbles of the same size which touch the probe. Next we will consider the population of bubbles of all sizes which touch the probe, given

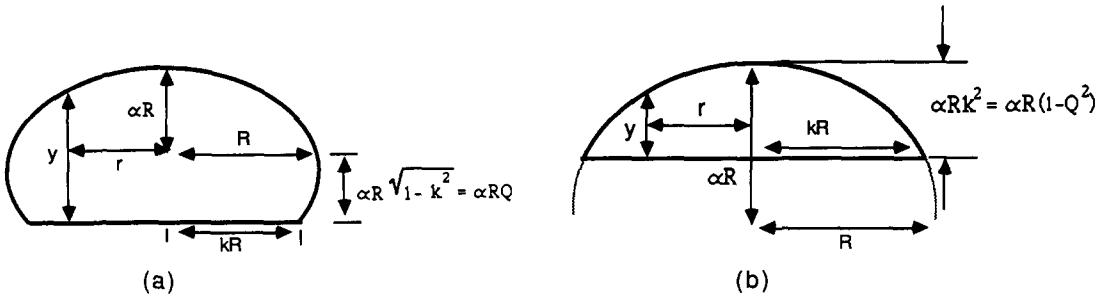

Figure 2. The vertical chord length, y, intersected by the probe, can be determined if the shape of the bubble and the distance from the bubble axis to the probe tip are known. (a) The shape illustrated here is the top greater section of an ellipsoid, representing a fluidized bed bubble. (b) The top lesser section of an ellipsoid represents a gas–liquid cap bubble. Notation for the text is provided in this figure.

by the probability density function $P(R)$. Considering this whole distribution, the probability that a bubble of size R will intersect the probe with a chord length y is then given by

$$P(y, R) = P(y \mid R)P(R). \qquad [4]$$

The probability of measuring a particular chord length y for *any* bubble size R in the system is

$$P(y) = \int_{-\infty}^{\infty} P(y, R)\,\mathrm{d}R$$

$$= \int_{-\infty}^{\infty} P(R)\,P(y \mid R)\,\mathrm{d}R. \qquad [5]$$

In practice the lower limit can be replaced by zero, and the upper by the largest bubble radius in the system, R_{max}. Equations [5] allows us to find the distribution of chord lengths, $P(y)$, for a given distribution of bubble sizes touching the probe, $P(R)$, provided that we know the bubble shape as given by [2]. An approximate scheme which allows us to reverse this procedure is discussed toward the end of this paper. Although [3] and [5] appear simple, they have fundamental implications in the analysis of specific bubble shapes and size distributions, as shown below.

SPECIFIC BUBBLE SHAPES

Several axisymmetic geometric shapes are considered in this paper as approximations of real bubbles found in multiphase systems. Some examples of the shapes of real bubbles are given below:

(i) Small spherical bubbles of gas are found in gas–liquid systems and liquid drops found in immiscible liquid–liquid systems. Both are modeled as spheres, and have been discussed by authors such as Batchelor (1977), Govier & Aziz (1972) and Harmathy (1960).

(ii) Larger bubbles (over 1.5 mm dia in air–water systems) assume the shape of an oblate spheroid or an ellipsoid, with a larger horizontal than axial dimension (Harmathy, 1960). These are modeled as ellipsoids.

(iii) Very large bubbles in liquids are cap-shaped (Hills 1975; Batchelor 1977). These can be modeled as the top lesser section of an ellipsoid or sphere.

(iv) In fluidized beds the bubble shape is often termed "spherical cap" [Werther (1974a) illustrates this] and is well-modeled by the top greater section of a sphere or ellipsoid, as shown in figure 2. The treatment of this general shape is the most difficult of all those mentioned above and receives greater attention than the others in the text which follows.

No attempt is made to model the shape of splitting or coalescing bubbles or of irregular voids found in gas–liquid froth flows (Taitel *et al.* 1980; Clark & Flemmer 1984). Data interpretation in such circumstances would be very difficult since the shape is not well-defined.

Let us consider a population of bubbles of known shape and of single size R. The shape chosen for analysis is the ellipsoid since it represents the most general, simply shaped bubble that one is likely to detect. The derivation of $P(y|R)$ for the greater upper section of the ellipsoid is given below and the results for other shapes are given in table 1.

Using the notation given in figure 2 we can write:

for $0 \leqslant r < kR$,

$$r^2 = R^2\left[1 - \left(\frac{y}{\alpha R} - \sqrt{1-k^2}\right)^2\right]$$

$$r^2 = R^2\left[1 - \left(\frac{y}{\alpha R} - Q\right)^2\right], \quad \text{where} \quad Q = \sqrt{1-k^2};$$

and for $kR \leqslant r \leqslant R$,

$$r^2 = R^2\left(1 - \frac{y^2}{4\alpha^2 R^2}\right);$$

therefore

$$\frac{dr}{dy} = \frac{R^2}{2r}\left(-\frac{2y}{4\alpha^2R^2}\right) = -\frac{y}{4\alpha^2 r}, \qquad kR < r \leqslant R,$$

$$= \frac{R^2}{2r}\left[-2\left(\frac{y}{\alpha R} - Q\right)\frac{1}{\alpha R}\right] = -\frac{R^2\left(\frac{y}{\alpha R} - Q\right)}{\alpha R r}, \qquad 0 \leqslant r \leqslant kR. \qquad [6]$$

Substituting [6] and [1] into [3] gives

$$P(y|R) = \frac{y}{2\alpha^2R^2}, \qquad 0 \leqslant y < 2\alpha QR,$$

$$= \frac{2}{\alpha^2R^2}(y - \alpha RQ), \qquad 2\alpha QR \leqslant y \leqslant \alpha R(1+Q), \qquad [7]$$

$$= 0, \qquad \text{otherwise.}$$

The conditional distributions for other bubble shapes are given in table 1.

The conditional distributions given in table 1 are also plotted in figures 3(a) and 3(b). It is interesting to note that for the greater upper sections of the ellipsoid and sphere there is a discontinuity in the conditional distribution. This step change in probability is expected since the value of dy/dr changes at this point, causing a step change in the probability density function.

Relationships Between Bubble Size and Chord Length Distributions

The object of this paper is to investigate the relationship between measured chord lengths and true bubble sizes. The ultimate goal is to be able to predict bubble size distributions for measured chord length distributions. This problem is addressed in the section concerning the backward transform. The following section focuses on the forward transform. This explains how the distribution of chord lengths can be generated with knowledge of the bubble shape and bubble size distribution.

Forward transform

Equation [5] provides the techniques for deducing the distribution of chord lengths for a given size distribution of bubbles affecting the probe. For the sake of simplicity we will assume that all the bubbles are geometrically similar and can be characterized by a single size parameter along with certain shape parameters (assumed constant for a given experiment). To demonstrate the procedure we will consider bubbles which can be approximated by the greater upper section of an ellipsoid

Table 1. Conditional chord length distributions for various shapes of bubble

Bubble shape	Parameters	Conditional chord length distribution	
Greater top section of an ellipsoid		$P(y\|R)=\frac{y}{2\alpha^2R^2}$	$0\leqslant y<2\alpha QR$
		$P(y\|R)=\frac{2(y-\alpha RQ)}{\alpha^2R^2}$	$2\alpha QR\leqslant y\leqslant\alpha R(1+Q)$
Ellipsoid	$Q=1$ $(k=0)$	$P(y\|R)=\frac{y}{2\alpha^2R^2}$	$0\leqslant y\leqslant 2\alpha R$
Greater top section of a sphere	$\alpha=1$	$P(y\|R)=\frac{y}{2R^2}$	$0\leqslant y<2QR$
		$P(y\|R)=\frac{2(y-RQ)}{R^2}$	$2QR\leqslant y\leqslant R(1+Q)$
Sphere	$\alpha=1$, $Q=1$ $(k=0)$	$P(y\|R)=\frac{y}{2R^2}$	$0\leqslant y\leqslant 2R$
Lesser top section of an ellipsoid		$P(y\|R)=\frac{2(y+\alpha RQ)}{\alpha^2R^2(1-Q^2)}$	$0\leqslant y\leqslant\alpha R(1-Q)$
Lesser top section of a sphere	$\alpha=1$	$P(y\|R)=\frac{2(y+RQ)}{R^2(1-Q^2)}$	$0\leqslant y\leqslant R(1-Q)$
Hemi ellipsoidal	$Q=0$ $(k=1)$	$P(y\|R)=\frac{2y}{\alpha^2R^2}$	$0\leqslant y\leqslant\alpha R$
Hemi spherical	$\alpha=1$, $Q=0$ $(k=1)$	$P(y\|R)=\frac{2y}{R^2}$	$0\leqslant y\leqslant R$

and we will further assume that the bubbles *affecting the probe* are uniformly distributed in size from 0 to R_{max}.

Thus

$$P(R)=\frac{1}{R_{max}},\qquad 0\leqslant R\leqslant R_{max},$$

and from [5]

$$P(y)=\int_{-\infty}^{\infty}P(y|R)\,P(R)\,\mathrm{d}R.$$

The above integral must be integrated in parts which may not be straightforward. The reason for this is that a chord length of a given size may come from the middle section of a small bubble or from the outer section of a large bubble. Figures 4(a) and 4(b) illustrate this method of solution.

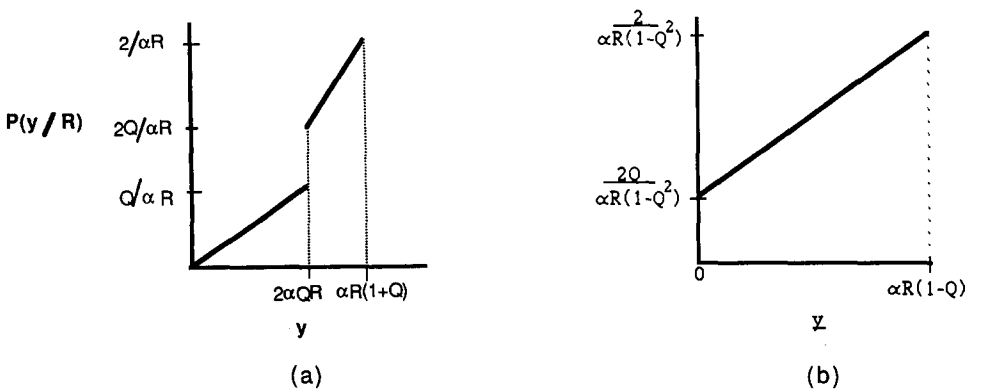

Figure 3. Plots of conditional distributions given in table 1. (a) Derived from the greater top section of an ellipsoid. (b) Derived from the lesser top section of an ellipsoid.

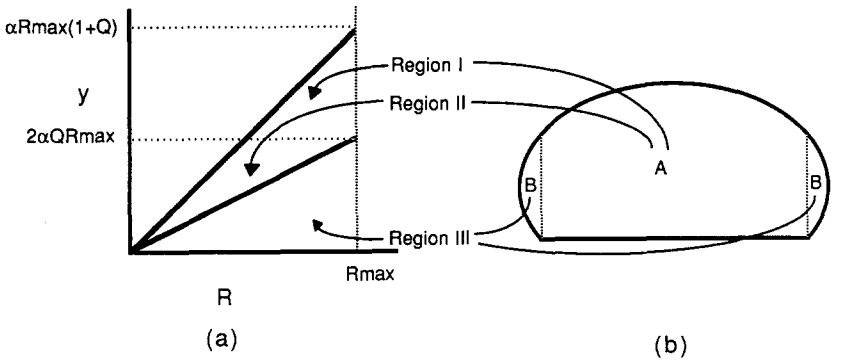

Figure 4. Relationships between chord lengths and bubble radius: (a) inner and outer regions of a bubble; (b) feasibility diagram.

Figure 4(a) represents the bubble with two outer sections (B) and one middle section (A). Figure 4(b) is a feasibility diagram for occurrence of chord length y vs bubble size R. The feasible region must be broken up into three regions:

I: represents the region from which chord lengths $> 2\alpha QR_{max}$ come from the middle section (A) of the bubble;
II: represents the region from which chord lengths $< 2\alpha QR_{max}$ come from the middle section (A) of the bubble;
III: represents the region from which chord lengths $< 2\alpha QR_{max}$ come from the outer sections (B) of the bubble.

Substituting the appropriate limits in [5] we obtain:

region I,

$$P(y) = \int_{y/\alpha(1+Q)}^{R_{max}} \frac{2}{\alpha^2 R^2}(y - \alpha RQ)\frac{1}{R_{max}}\,dR; \qquad [8]$$

region II,

$$P(y) = \int_{y/\alpha(1+Q)}^{y/2\alpha Q} \frac{2}{\alpha^2 R^2}(y - \alpha RQ)\frac{1}{R_{max}}\,dR; \qquad [9]$$

region III,

$$P(y) = \int_{y/2\alpha Q}^{R_{max}} \frac{y}{2\alpha^2 R^2}\frac{1}{R_{max}}\,dR. \qquad [10]$$

Performing the integrations in [8]–[10] and combining we obtain

$$P(y) = \frac{1}{\alpha^2 R_{max}}\left[2\alpha(1-Q) + \alpha Q - \frac{y}{2R_{max}} - 2\alpha Q \ln\frac{(1+Q)}{2Q}\right], \qquad 0 \leqslant y < 2\alpha R_{max} Q,$$

$$P(y) = \frac{1}{\alpha^2 R_{max}}\left[2\alpha(1+Q) - \frac{2y}{R_{max}} - 2\alpha Q \ln\frac{\alpha R_{max}(1+Q)}{y}\right], \qquad 2\alpha R_{max} \leqslant y \leqslant \alpha R_{max}(1+Q). \qquad [11]$$

Equation [11] represents the distribution of chord lengths (y) resulting from sampling bubbles with the shape of the greater upper section of an ellipsoid, and assuming the bubbles to be uniformly distributed in the region of the probe.

Results for other bubble shapes are given in table 2, along with the results for the case when bubbles are uniformly distributed across the bed. For this latter case

$$P_s(R) = \frac{1}{R_{max}}, \qquad 0 \leqslant R \leqslant R_{max},$$

and

$$P(R) = \frac{3R^2}{R_{\max}^3}, \qquad 0 \leqslant R \leqslant R_{\max} \qquad [12]$$

(assuming $R_{\max} < R_{\text{bed}}/2$).

We are in no way restricted to using uniform bubble size distributions since the definition in [5] is quite general. However the integrations required to evaluate $P(y)$ become increasingly more complex for more complicated bubble size distributions. For example, if $P(R)$ is a triangular distribution then to obtain $P(y)$ for the greater upper section of an ellipsoid the integration requires the evaluation of 7 or 8 separate integrals. At this point it is more convenient to evaluate the distributions numerically.

Backward transform

We now focus on the problem of generating the bubble size distribution $P(R)$ given the distribution of chord lengths $P(y)$. In practice we will always measure the distribution of chord lengths and try to deduce the bubble size distribution, hence the backward transform is of great importance in experimental data analysis.

It should be pointed out that the true bubble size distribution is never (or rarely ever) known. For well-behaved distributions the following approximate method will yield satisfactory results. There are, however, problems with some distributions and these are discussed briefly at the end of this section.

Consider a set of data consisting of n observations of chord lengths y. Let us divide the chord lengths into m equal length partitions such that

$$y_i = y_{\max} - (i + \tfrac{1}{2})\,\Delta y, \qquad 0 \leqslant i \leqslant m - 1,$$

where

$$\Delta y = \frac{y_{\max}}{m}.$$

Then an approximation to the probability of finding a chord length y between y_i and y_{i+1}, $W(y_i < y < y_{i+1})$, is given by

$$W(y_i < y < y_{i+1}) = \frac{\text{Number of observations of chord lengths between } y_i \text{ and } y_{i+1}}{\text{Total number of observations, } n}. \qquad [13]$$

From [5] we have

$$\begin{aligned} W(y_i < y < y_{i+1}) &= \int_{y_i}^{y_{i+1}} P(y)\,\mathrm{d}y = \int_{y_i}^{y_{i+1}} \int_0^{R_{\max}} P(y\,|\,R)P(R)\,\mathrm{d}R\,\mathrm{d}y \\ &= \int_{y_i}^{y_{i+1}} \left[\int_0^{R_{m-1}} P(y\,|\,R)P(R)\,\mathrm{d}R + \int_{R_{m-1}}^{R_{m-2}} (P(y\,|\,R)P(R)\,\mathrm{d}R + \cdots \right. \\ &\quad \left. + \int_{R_1}^{R_0} P(y\,|\,R)P(R)\,\mathrm{d}R \right] \mathrm{d}y \simeq \int_{y_i}^{y_{i+1}} \sum_{j=0}^{m-1} P(y\,|\,R_j)P(R_j)\Delta R\,\mathrm{d}y \\ &\simeq \sum_{j=0}^{m-1} \int_{y_i}^{y_{i+1}} P(y\,|\,R_j)\,\mathrm{d}y\,P(R_j)\Delta R. \end{aligned}$$

Hence

$$W_i = W(y_i < y \leqslant y_{i+1}) \simeq \sum_{j=0}^{m-1} C_{i,j} P(R_j)\Delta R, \qquad [14]$$

Table 2. Chord length distributions for various shapes of bubbles

Bubble shape	Parameters	Distribution of chord lengths for different bubble size distributions	
		(A) Uniform distribution at probe $P(R) = \frac{1}{R_{max}}$ $0 \leqslant R \leqslant R_{max}$	
Greater upper section of an ellipsoid		$P(y) = \frac{1}{\alpha^2 R_{max}} \left\{ 2\alpha(1-Q) + \alpha Q - \frac{y}{2R_{max}} - 2\alpha Q \ln\left[\frac{(1+Q)}{2Q}\right] \right\}$	$0 \leqslant y < 2\alpha R_{max} Q$
		$= \frac{1}{\alpha^2 R_{max}} \left\{ 2\alpha(1+Q) - \frac{2y}{R_{max}} - 2\alpha Q \ln\left[\frac{\alpha R_{max}(1+Q)}{y}\right] \right\}$	$2\alpha R_{max} Q \leqslant y \leqslant \alpha R_{max}(1+Q)$
Lesser upper section of an ellipsoid		$P(y) = \frac{2}{\alpha R_{max}}(1-Q^2) \left\{ Q \ln\left[\frac{\alpha R_{max}(1-Q)}{y}\right] - \frac{y}{\alpha R_{max}} + (1-Q) \right\}$	$0 \leqslant y \leqslant \alpha R_{max}(1-Q)$
Ellipsoid	$Q = 1$ $(k = 0)$	$P(y) = \frac{1}{2\alpha^2 R_{max}^2} \left[(2\alpha R_{max} - y) \right]$	$0 \leqslant y \leqslant 2\alpha R_{max}$
Greater upper section of a sphere	$\alpha = 1$	$P(y) = \frac{1}{R_{max}} \left\{ 2 - Q - \frac{y}{2R_{max}} - 2Q \ln\left[\frac{(1+Q)}{2Q}\right] \right\}$	$0 \leqslant y < 2R_{max} Q$
		$= \frac{1}{R_{max}} \left\{ 2(1+Q) - \frac{2y}{R_{max}} - 2Q \ln\left[\frac{(1+Q)R_{max}}{y}\right] \right\}$	$2R_{max} Q \leqslant y \leqslant R_{max}(1+Q)$
Lesser upper section of a sphere	$\alpha = 1$	$P(y) = \frac{2}{R_{max}} \frac{1}{(1-Q)} \left[Q \ln \frac{R_{max}(1-Q)}{y} - \frac{y}{R_{max}} + (1-Q) \right]$	$0 \leqslant y \leqslant R_{max}(1-Q)$
Sphere	$\alpha = 1$, $Q = 1$ $(k = 0)$	$P(y) = \frac{1}{2R_{max}^2}(2R_{max} - y)$	$0 \leqslant y \leqslant 2R_{max}$

(B) Uniform distributions in system $P(R) = \dfrac{3R^2}{R_{max}^3}$ $0 \leqslant R \leqslant R_{max}$

Greater upper section of an ellipsoid		$P(y) = \dfrac{6}{\alpha^2 R_{max}^3}\left\{\dfrac{yR_{max}}{4} + \dfrac{y^2}{4\alpha Q} + \dfrac{[Q-2(1+Q)]\,y^2}{2\alpha(1+Q)^2}\right\}$	$0 \leqslant y < 2\alpha R_{max} Q$
		$= \dfrac{6}{\alpha^2 R_{max}^3}\left\{yR_{max} - \dfrac{\alpha Q R_{max}^2}{2} + \dfrac{[Q-2(1+Q)]}{2\alpha(1+Q)^2}y^2\right\}$	$2\alpha R_{max} Q \leqslant y \leqslant \alpha R_{max}(1+Q)$
Lesser upper section of an ellipsoid		$P(y) = \dfrac{3}{R_{max}^3(1-Q^2)\alpha}\left[\dfrac{2R_{max}\,y}{\alpha} + QR_{max}^2 - \dfrac{(2+Q)\,y^2}{(1-Q)^2\alpha^2}\right]$	$0 \leqslant y \leqslant \alpha R_{max}(1-Q)$
Ellipsoid	$Q = 1$ $(k = 0)$	$P(y) = \dfrac{6}{\alpha^2 R_{max}^3}\left(\dfrac{yR_{max}}{4} - \dfrac{y^2}{8\alpha}\right)$	$0 \leqslant y \leqslant 2\alpha R_{max}$
Greater upper section of an sphere	$\alpha = 1$	$P(y) = \dfrac{6}{R_{max}^3}\left\{\dfrac{yR_{max}}{4} + \dfrac{y^2}{4Q} + \dfrac{[Q-2(1+Q)]}{2(1+Q)^2}y^2\right\}$	$0 \leqslant y < 2R_{max} Q$
		$= \dfrac{6}{R_{max}^3}\left\{yR_{max} - \dfrac{QR_{max}}{2} + \dfrac{[Q-2(1+Q)]}{2(1+Q)^2}y^2\right\}$	$2R_{max} Q \leqslant y \leqslant R_{max}(1+Q)$
Lesser upper section of a sphere	$\alpha = 1$	$P(y) = \dfrac{3}{R_{max}^3}(1-Q^2)\left[2R_{max}\,y + QR_{max}^2 - \dfrac{(2+Q)\,y^2}{(1-Q)^2}\right]$	$0 \leqslant y \leqslant R_{max}(1-Q)$
Sphere	$\alpha = 1$, $Q = 1$ $(k = 0)$	$P(y) = \dfrac{6}{R_{max}^3}\left(\dfrac{yR_{max}}{4} - \dfrac{y^2}{8}\right)$	$0 \leqslant y \leqslant 2R_{max}$

where

$$C_{i,j} = \int_{y_i}^{y_{i+1}} P(y \mid R_j)\, dy$$

and

$$R_j = R_{\max} - j\Delta R, \qquad 0 \leqslant j \leqslant m-1,$$

with

$$\Delta R = \frac{R_{\max}}{m} = \frac{y_{\max}}{\alpha(1+Q)m}.$$

Equation [14] can be used to construct the following triangular matrix form:

$$W_0 = C_{0,0}P(R_0)\Delta R$$
$$W_1 = C_{1,0}P(R_0)\Delta R + C_{1,1}P(R_1)\Delta R$$
$$\vdots$$
$$W_{m-1} = C_{m-1,0}P(R_0)\Delta R + C_{m-1,1}P(R_1)\Delta R + \cdots + C_{m-1,m-1}P(R_{m-1})\Delta R.$$

The triangularity occurs because $C_{i,j}$ is zero when $i < j$, i.e. a chord length y_i can only come from a bubble of radius R_i or greater (R_{i-1}, R_{i-2} etc.). For a known bubble shape $C_{i,j}$ is known and

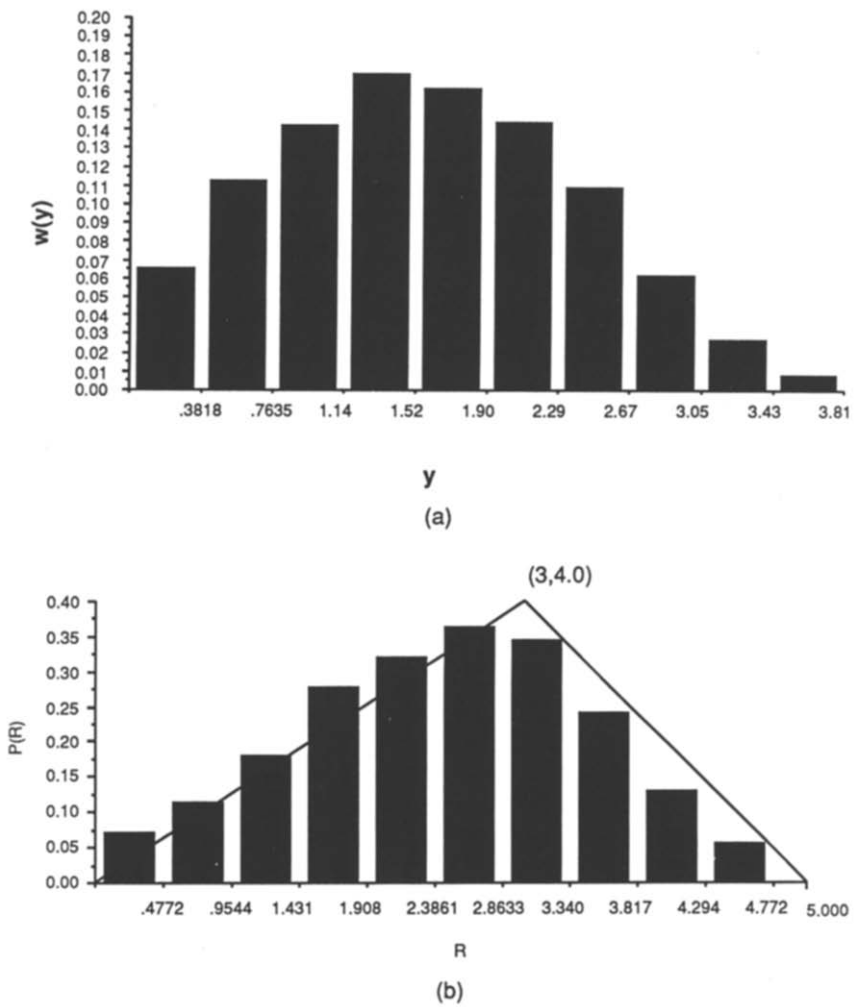

Figure 5. A simulated experiment was used to verify the back transform scheme: (a) the generated probability histogram of chord lengths; (b) the original bubble size distribution (used to generate the chord lengths) and the size distribution found from the chord length distribution are compared.

the W_i are calculated from the chord length data. Thus the above matrix can be solved sequentially to yield the unknown $P(R_i)$. More sophisticated solution algorithms are certainly possible but the equations given above will yield accurate results provided that the intervals between between y_1, y_2 etc. are not too small.

Illustrative example

Five thousand chord length observations were generated synthetically using Monte Carlo simulation. A triangular bubble size distribution was assumed with mode = 3 and range $0 \leqslant R \leqslant 5$: Bubble shape was assumed to be the greater upper section of an ellipsoid with $\alpha = 0.5$ and $k = 0.8$. The generated distribution of chord lengths is shown in figure 5(a). The backward transformation was carried out on the data and the resulting probability density function for R is compared with the actual bubble size distribution in figure 5(b). This comparison of the actual distribution and the backward transformation is good and illustrates the utility of this technique.

This worked example with 10 subdivisions in bubble size gives accurate results. If the number of subdivisions is increased beyond a certain point then for a fixed sample size of chord lengths the backward transform becomes unstable yielding irregular and sometimes negative $P(R)$ values. This instability results from the fact that for each subdivision there must exist a representative number of data points within the region. Therefore if one requires more subdivisions then one must take more data.

Very irregular (multimodal) bubble size distributions may occur in practice and these can be difficult to treat using the above backward transform. The presence of multimodal features in the chord length distribution would nearly always occur in these cases and thus inspection of the raw data can give insight into such problems.

Acknowledgements—N. N. Clark is grateful for support from the West Virginia University/Industry/National Science Foundation Center for Fluidization Research and from a West Virginia University Senate Research Grant. R. Turton is grateful for support from the National Science Foundation, Award No. CBT-8657548.

REFERENCES

ATKINSON, C. M. & CLARK, N. N. 1986a A gas sampling system for high temperature fluidized beds. In *Proc. 11th Powder Bulk Solids Conf.*, Rosemont, Ill., pp. 444–454.

ATKINSON, C. M. & CLARK, N. N. 1986b Analysis of fluidized bed behavior using probes. In *Proc. 11th Powder Bulk Solids Conf.*, Rosemont, Ill., pp. 437–443.

ATKINSON, C. M. & CLARK, N. N. 1988 Gas sampling from fluidized beds: a novel probe system. *Powder Technol.* In press.

BATCHELOR, G. K. 1977 *An Introduction to Fluid Dynamics*. Cambridge Univ. Press, London.

BUCHHOLZ, R., ZAKRZEWSKI, W. & SCHUGERL, K. 1981 Techniques for determining the properties of bubbles in bubble columns. *Int. chem. Engng* **21,** 180–187.

BURGESS, J. M., FANE, A. G. & FELL, C. J. D. 1981 Application of an electroresistivity probe technique to a two dimensional fluidized bed. *Trans. Instn chem. Engrs* **60,** 249–252.

CHEREMISINOFF, N. P. 1986 Review of experimental methods for studying hydrodynamics of gas–solid fluidized bed. *Ind. Engng Chem. Process Des. Dev.* **25,** 329–351.

CLARK, N. N. & FLEMMER, R. L. C. 1984 The bubble to slug flow transition in gas–liquid upflow and downflow. *J. Pipelines* **5,** 53–65.

FITZGERALD, T. J. 1979 Review of instrumentation for fluidized beds. Presented at a workshop, Rensselaer Polytechnic Inst., Troy, N.Y.

FLEMMER, R. L. C. 1984 A Pneumatic probe to detect gas bubbles in fluidized beds. *Ind. Engng Chem. Fundam.* **23,** 113–115.

GALAUP, J. P. 1975 Doctoral Thesis, Scientific & Medical University of Grenoble, France.

GOVIER, G. W. & AZIZ, K. 1972 *The Flow of Complex Mixtures in Pipes*. Van Nostrand-Reinhold, New York.

GUNN, D. J. & AL-DOORI, H. H. 1985 The measurement of bubble flows in fluidized beds by electrical probe. *Int. J. Multiphase Flow* **11,** 535–551.

HARMATHY, T. Z. 1960 Velocity of large drops and bubbles in media of infinite or restricted extent. *AIChE Jl* **6,** 281–288.

HERRINGE, R. A. & DAVIS, M. R. 1978 Flow structure and distribution effects in gas–liquid mixture flows. *Int. J. Multiphase Flow* **4,** 461–468.

HILLS, J. H. 1975 The rise of a large bubble through a stream of smaller ones. *Trans. Instn chem. Engrs* **53,** 224–233.

KOIDE, K., MOROOKA, S., UEYAMA, K., MATSUURA, A., YAMASHITA, F., IWAMOTO, S., KATO, Y., INOUE, H., SHIGETA, M., SUZUKI, S. & AKEHATA, T. 1979 Behavior of bubbles in large scale bubble column. *J. chem. Engng Japan* **12,** 98–104.

SEKOGUCHI, K., FUKUI, H., MATSUOKA, T. & NISHIKAWA, K. 1975 Investigation into the statistical characteristics of bubbles in two-phase flow. *Bull. JSME* **18,** 391–404.

SERIZAWA, A., KATAOKA, I. & MICHIYOSHI, I. 1975 Turbulence structure of air–water bubble flow. *Int. J. Multiphase Flow* **2,** 225–259.

TAITEL, Y., BARNEA, B. & DUKLER, A. E. 1980 Modelling flow pattern transitions for steady upward gas–liquid flow. *AIChE Jl* **26,** 345–354.

WERTHER, J. 1974a Bubbles in gas fluidized beds–Part 1. *Trans. Instn chem. Engrs* **52,** 149–159.

WERTHER, J. 1974b Bubbles in gas fluidized beds–Part II. *Trans. Instn chem. Engrs* **52,** 160–169.

WERTHER, J. & MOLERUS, O. 1973 The local structure of gas fluidized beds. *Int. J. Multiphase Flow* **1,** 103–122.

YAMASHITA, F., MORI, Y. & FUJITA, S. 1979 Sizes and size distributions of bubbles in a bubble column. *J. chem. Engng Japan* **12,** 5–9.